Intercomparison of Surface Temperatures from AIRS, MERRA, and MERRA-2 with NOAA and GC-Net Weather Stations at Summit, Greenland

THOMAS J. HEARTY III,[a,b] JAE N. LEE,[c,d] DONG L. WU,[d] RICHARD CULLATHER,[e,f] JOHN M. BLAISDELL,[g,h] JOEL SUSSKIND,[h] AND SOPHIE M. J. NOWICKI[h]

[a] *Stinger Ghaffarian Technologies, Greenbelt, Maryland*
[b] *Goddard Earth Sciences Data Information and Services Center, NASA Goddard Space Flight Center, Greenbelt, Maryland*
[c] *Joint Center for Earth Systems Technology, University of Maryland, Baltimore County, Baltimore, Maryland*
[d] *Climate and Radiation Laboratory, NASA Goddard Space Flight Center, Greenbelt, Maryland*
[e] *Earth System Science Interdisciplinary Center, University of Maryland, College Park, College Park, Maryland*
[f] *Global Modeling and Assimilation Office, NASA Goddard Space Flight Center, Greenbelt, Maryland*
[g] *Science Applications International Corporation, Greenbelt, Maryland*
[h] *Earth Sciences Division, NASA Goddard Space Flight Center, Greenbelt, Maryland*

(Manuscript received 28 July 2017, in final form 14 February 2018)

ABSTRACT

The surface skin and air temperatures reported by the Atmospheric Infrared Sounder/Advanced Microwave Sounding Unit-A (AIRS/AMSU-A), the Modern-Era Retrospective Analysis for Research and Applications (MERRA), and MERRA-2 at Summit, Greenland, are compared with near-surface air temperatures measured at National Oceanic and Atmospheric Administration (NOAA) and Greenland Climate Network (GC-Net) weather stations. The AIRS/AMSU-A surface skin temperature (TS) is best correlated with the NOAA 2-m air temperature (T2M) but tends to be colder than the station measurements. The difference may be the result of the frequent near-surface temperature inversions in the region. The AIRS/AMSU-A surface air temperature (SAT) is also correlated with the NOAA T2M but has a warm bias during the cold season and a larger standard error than the surface temperature. The extrapolation of the temperature profile to calculate the AIRS SAT may not be valid for the strongest inversions. The GC-Net temperature sensors are not held at fixed heights throughout the year; however, they are typically closer to the surface than the NOAA station sensors. Comparing the lapse rates at the two stations shows that it is larger closer to the surface. The difference between the AIRS/AMSU-A SAT and TS is sensitive to near-surface inversions and tends to measure stronger inversions than both stations. The AIRS/AMSU-A may be sampling a thicker layer than either station. The MERRA-2 surface and near-surface temperatures show improvements over MERRA but little sensitivity to near-surface temperature inversions.

1. Introduction

The surface skin temperature (TS) and air temperature (SAT) records over the Greenland ice sheet are important climate indicators. The SAT has shown the rate of warming over Greenland to be 6 times the global average (McGrath et al. 2013), while the TS is the fundamental driving force of the rapid Greenland ice sheet (GrIS) melt in recent years. The warming TS has led to increased surface melting and runoff, along with increased discharge of glacier ice to the ocean (Hall et al. 2008), likely through transferring surface melt to the ice sheet bed via moulins and crevasses (Zwally et al. 2002). The TS is also used as a key input variable to ice sheet models in assessing the ice volume of Greenland (Bindschadler et al. 2013; Alley and Joughin 2012).

Despite its importance as a climate indicator, the SAT over the GrIS is only directly measured at a sparse set of locations (e.g., Steffen et al. 1996). Although the stations provide accurate temperature measurements, they require routine maintenance to avoid being covered in

Corresponding author: Thomas J. Hearty, thomas.j.hearty@nasa.gov

DOI: 10.1175/JAMC-D-17-0216.1

TABLE 1. NOAA and GC-Net station locations.

Station	Lon	Lat
NOAA	−38.48	72.5800
GC-Net	−38.50	72.5794
Average	−38.49	72.5797

snow, which can cause discontinuities in the data records. Observations from space can provide a useful complement to the ground-based observations since they provide greater spatial coverage. For example, a recent study used Atmospheric Infrared Sounder/Advanced Microwave Sounding Unit-A (AIRS/AMSU-A) level-3 surface temperature as a boundary layer model input to estimate the vapor flux over Greenland (Boisvert et al. 2017). Hall et al. (2008) reviewed measurements from orbiting IR sensors, and found that ETM+, ASTER, and MODIS all had comparable performance on remotely sensing TS over Greenland. Although these sensors have the advantage of a relatively high spatial resolution, they are limited to clear-sky conditions and can have difficulty screening out nighttime clouds that can cause erroneous TS measurements (Hall et al. 2013).

Shuman et al. (2014) have shown that the MODIS ice surface temperature (IST) can be matched with the station 2-m temperature with a seasonally dependent offset. However, they also point out that the MODIS IST observations have both a scan angle dependence and a solar zenith angle dependence. In this paper we examine the TS and SAT reported in the AIRS/AMSU-A version-6 level-2 products that have been collocated in time and space with NOAA and Greenland Climate Network (GC-Net) station observations from Summit, Greenland (72.6°N, 38.5°W). We also examine atmospheric reanalysis surface temperature and near-surface air temperature estimates from the Modern-Era Retrospective Analysis for Research and Applications (MERRA; Rienecker et al. 2011) and its version-2 successor (MERRA-2; Bosilovich et al. 2016), which have been collocated in space and time with AIRS/AMSU-A

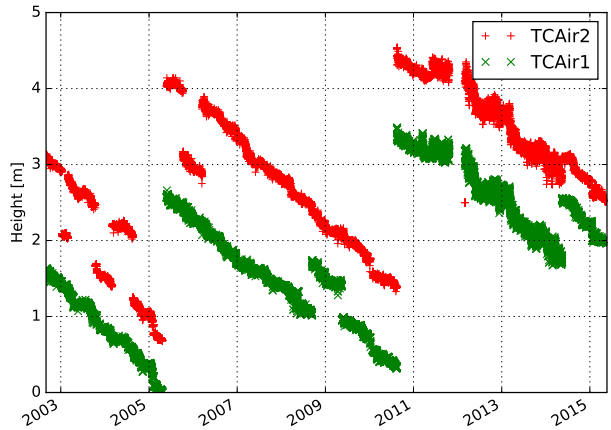

FIG. 1. A time series of the height of the GC-Net temperature sensors.

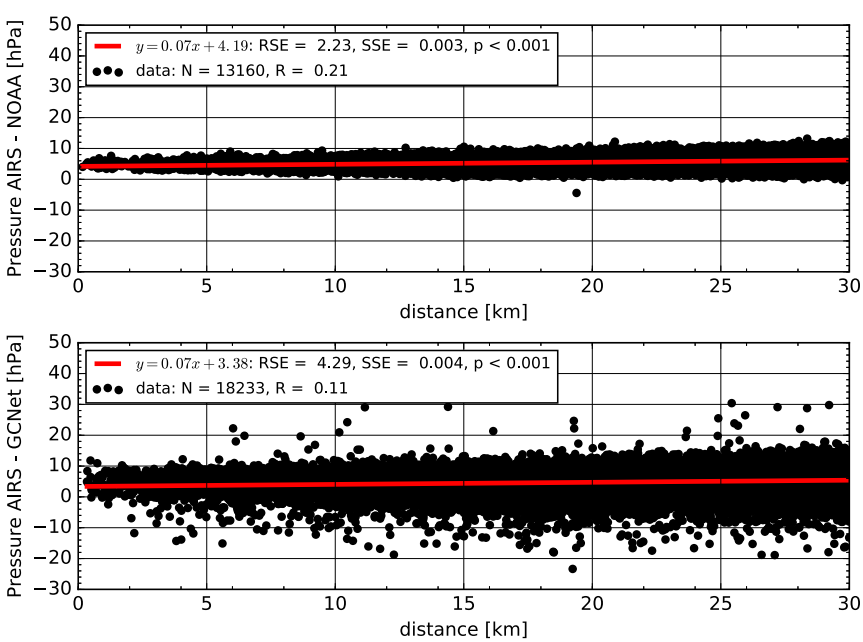

FIG. 2. The difference between the surface pressure assumed by AIRS/AMSU-A algorithm and the pressure recorded at (top) NOAA and (bottom) GC-Net Summit stations.

TABLE 2. Summary of temperature comparisons (°C).

Ordinate	Abscissa	Linear parameters	RSE	SSE	p	N points	R	Figure
AIRS/AMSU-A TS	NOAA T2M	$y = 1.00x - 2.44$	2.84	0.002	<0.001	11 003	0.98	Fig. 3
AIRS/AMSU-A TS	GCNet TCAir1	$y = 0.97x - 2.99$	3.29	0.002	<0.001	17 307	0.97	Fig. 3
AIRS/AMSU-A SAT	NOAA T10M	$y = 0.94x - 3.12$	4.06	0.003	<0.001	11 820	0.93	Fig. 4
AIRS/AMSU-A SAT	NOAA T2M	$y = 0.80x - 4.35$	3.79	0.003	<0.001	12 537	0.94	Fig. 4
MSA T10M	NOAA T10M	$y = 0.78x - 7.08$	2.69	0.002	<0.001	12 163	0.95	Fig. 5
MSA T2M	NOAA T2M	$y = 0.69x - 8.92$	2.07	0.002	<0.001	12 921	0.95	Fig. 5
MSA TS	AIRS/AMSU-A TS	$y = 0.85x - 8.23$	4.53	0.003	<0.001	19 299	0.92	Fig. 5
M2SA T10M	NOAA T10M	$y = 0.90x - 3.71$	2.64	0.002	<0.001	12 307	0.97	Fig. 6
M2SA T2M	NOAA T2M	$y = 0.81x - 5.06$	3.09	0.002	<0.001	13 065	0.96	Fig. 6
M2SA TS	AIRS/AMSU-A TS	$y = 0.95x - 1.55$	3.78	0.002	<0.001	19 430	0.95	Fig. 6

observations at Summit. Since strong temperature inversions are common in the Arctic (e.g., Devasthale et al. 2010), we also examine near-surface temperature inversions at Summit.

2. Observations and analysis

This study utilizes prototypes of data subsetting and aggregation capabilities developed at the Goddard Earth Science Data Information and Services Center (GES DISC) that enable direct comparisons of satellite and reanalysis datasets with any point source (e.g., ground station measurements). In this study, AIRS/AMSU-A, MERRA, and MERRA-2 data are matched in time and space with Greenland station observations. All linear fits presented in this paper were performed using the linregress program in the SciPy statistics package and the figures are annotated with the linear fit parameters, the residual standard error RSE, the slope standard error SSE, the P value p, the number of points N, and the correlation coefficient R.

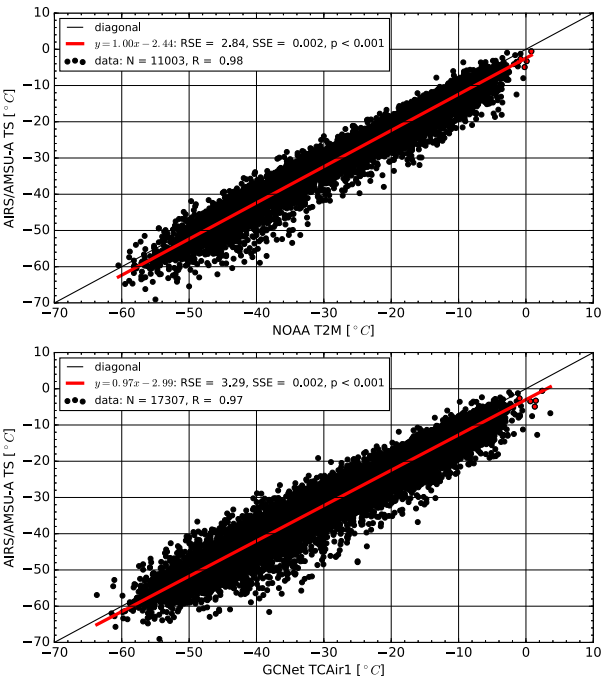

FIG. 3. AIRS TS is compared with (top) NOAA T2M and (bottom) GC-Net TCAir1 temperatures. The station temperatures above 0°C are associated with a melt event that occurred in the summer of 2012 that will be discussed further in section 4c. The red symbols correspond to AIRS observations that were classified as "land" by the AMSU-A surface classification algorithm.

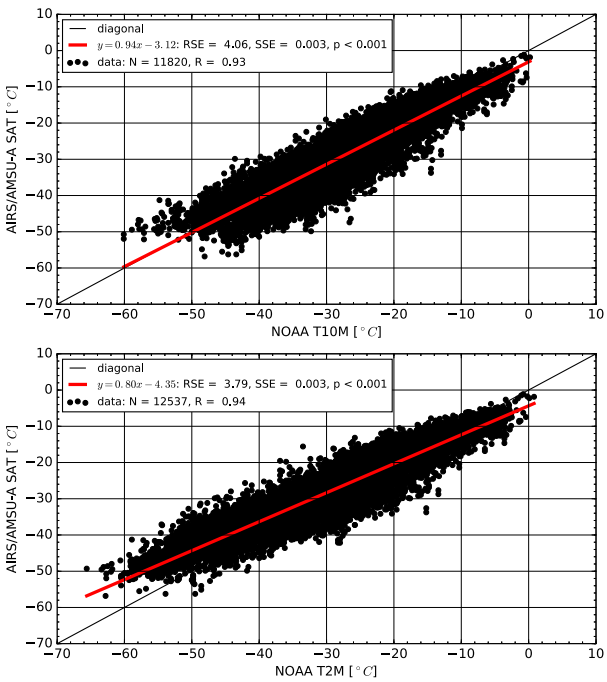

FIG. 4. AIRS SAT is compared with NOAA (top) T10M and (bottom) T2M temperatures.

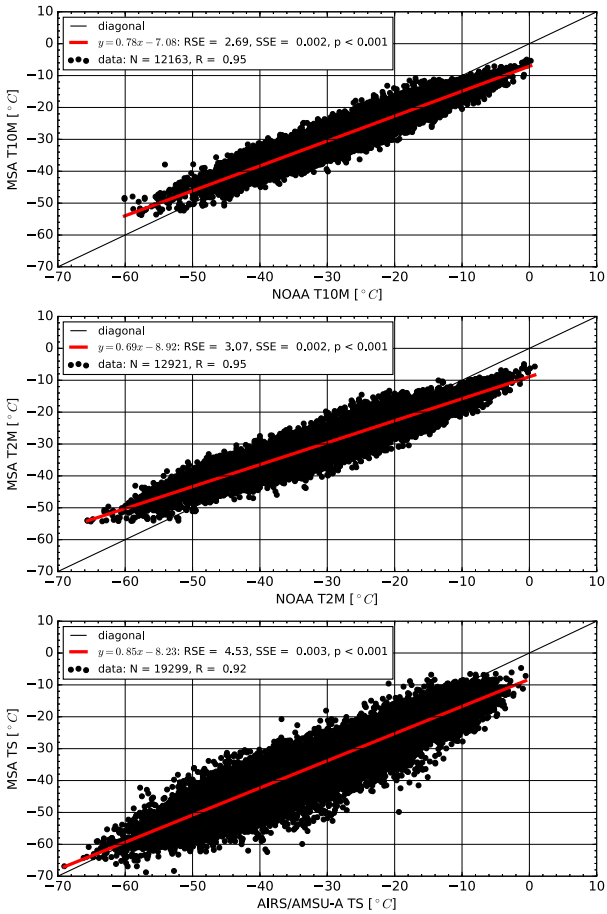

FIG. 5. MSA near-surface air temperatures (top) T10M and (middle) T2M are compared to their respective NOAA station temperatures, and (bottom) the MERRA surface temperature TS is compared to the AIRS/AMSU-A surface temperature.

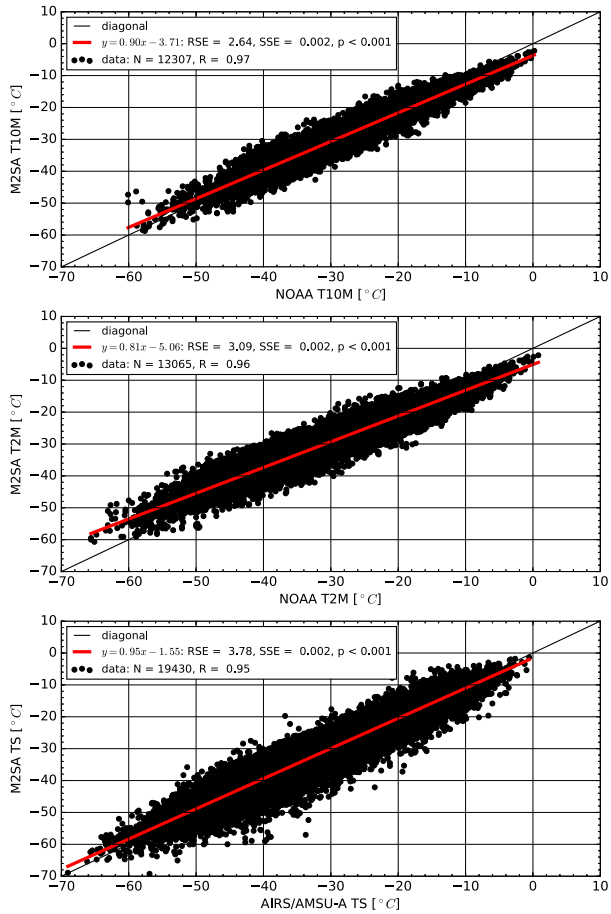

FIG. 6. As in Fig. 5, but for M2SA.

a. Greenland Summit stations

The in situ temperature and pressure measurements used in this study are hourly averages of sensors at the NOAA and GC-Net (Steffen et al. 1996) weather stations at Summit. The GC-Net data included in this study span from 1 September 2002 through 22 May 2015, with a few periods of missing data, and the NOAA data span from 25 June 2008 through 17 April 2016. The locations of the two stations and the average location are listed in Table 1. We use the average location of the two stations to identify the nearest AIRS/AMSU-A, MERRA, and MERRA-2 data for comparisons.

The NOAA station air temperature measurements are maintained at 2 (T2M) and 10 m (T10M) above the surface. The height of the GC-Net temperature sensors (TCAir1 and TCAir2) are recorded but not maintained at fixed heights above the surface throughout the year (see Fig. 1). Over the period examined, the median height of the TCAir1 sensor was 1.7 m, with 90% of the measurements between 0.4 and 3.2 m, and the median height of the TCAir2 sensor was 2.9 m, with 90% of the measurements between 1.2 and 4.2 m. The median distance between the GC-Net sensors was 1.1 m, with 90% of the measurements made with a sensor separation between 0.6 and 1.6 m.

b. AIRS/AMSU-A

The AIRS/AMSU-A suite of instruments observes Earth from aboard the *Aqua* spacecraft at an altitude of ~705 km in a near-polar sun-synchronous orbit with an inclination of 98.2° (Parkinson 2003) and a 98.8-min orbital period. The ascending nodes of the orbit (i.e., when the spacecraft is moving toward the north) cross the equator ~1330 local time, and the descending nodes of the orbit (when the spacecraft is moving toward the south) cross the equator ~0130 local time. Since the AIRS/AMSU-A instruments scan between ±49° about nadir with a swath width of ~1650 km (Aumann et al. 2003),

TABLE 3. Summary of geometrical and environmental observing conditions.

Abscissa	Linear parameters	RSE	SSE	p	N points	R	Figure
	AIRS/AMSU-A TS–NOAA T2M (°C) (ordinate)						
Distance (km)	$y = -0.01x - 2.24$	2.84	0.004	0.047	11 003	−0.02	Fig. 7
Time (s)	$y = -0.00x - 2.23$	2.84	0.000	<0.001	11 003	−0.03	Fig. 7
Scan angle (°)	$y = -0.00x - 2.35$	2.84	0.002	0.430	11 003	−0.01	Fig. 7
Solar zenith angle (°)	$y = -0.06x - 2.24$	2.39	0.003	<0.001	4956	−0.29	Fig. 8
AIRS/AMSU-A cloud fraction	$y = -0.38x - 2.28$	2.84	0.1	<0.001	10 137	−0.04	Fig. 8
NOAA T10M–T2M (°C)	$y = -0.14x - 1.98$	2.8	0.008	<0.001	10 137	−0.18	Fig. 8
	AIRS/AMSU-A SAT–NOAA T2M (°C) (ordinate)						
Distance (km)	$y = 0.02x + 1.09$	4.63	0.006	<0.001	12 537	0.03	Fig. 9 (left)
Time (s)	$y = 0.00x + 1.33$	4.63	0.000	0.015	12 537	0.02	Fig. 9 (left)
Scan angle (°)	$y = 0.03x + 0.65$	4.60	0.003	<0.001	12 537	0.11	Fig. 9 (left)
Solar zenith angle (°)	$y = 0.11x - 6.29$	3.56	0.004	<0.001	5188	0.34	Fig. 10 (left)
AIRS/AMSU-A cloud fraction	$y = -7.42x - 3.15$	4.22	0.14	<0.001	11 632	−0.44	Fig. 10 (left)
NOAA T10M–T2M (°C)	$y = 0.68x - 0.50$	3.9	0.009	<0.001	11 632	0.56	Fig. 10 (left)
	AIRS/AMSU-A SAT–NOAA T10M (°C) (ordinate)						
Distance (km)	$y = 0.01x - 1.71$	4.11	0.005	0.082	11 820	0.02	Fig. 9 (right)
Time (s)	$y = 0.00x - 1.59$	4.11	0.000	0.327	11 820	0.01	Fig. 9 (right)
Scan angle (°)	$y = 0.03x - 2.35$	4.08	0.003	<0.001	11 820	0.11	Fig. 9 (right)
Solar zenith angle (°)	$y = 0.01x - 1.03$	3.29	0.004	0.016	5188	0.04	Fig. 10 (right)
AIRS/AMSU-A cloud fraction	$y = -2.37x - 1.01$	4.04	0.134	<0.001	11 632	−0.16	Fig. 10 (right)
NOAA T10M–T2M (°C)	$y = -0.32x - 0.50$	3.90	0.009	<0.001	11 632	−0.31	Fig. 10 (right)

adjacent orbits can sample the same location near the poles. Because of this wide swath, typically, there are 3–4 AIRS/AMSU-A observations at Summit per day.

The AIRS hyperspectral infrared and AMSU-A multichannel microwave instruments provide a unique capability of measuring surface and atmosphere temperature and water vapor simultaneously in all-sky conditions at ~50-km resolution (Susskind et al. 2014). The AIRS/AMSU-A algorithm employs the cloud-cleared radiance approach iteratively and produces the best fit spectrum to the cloud cleared radiances. Using the nine 15-km hyperspectral IR measurements inside a 50-km multichannel microwave scene, the retrieval algorithm is able to take advantage of cloud inhomogeneity in a smooth clear-sky background to estimate what the cloud-clear radiances should be as the cloud fraction approaches zero, even where all nine footprints are cloudy. As a result, the retrieval of surface properties (e.g., skin temperature) can still be obtained when cloud fractions are moderately low or fluctuate within the 50-km AMSU-A footprint. However, the error would increase when all nine IR footprints are heavily covered by clouds with few inhomogeneities. In this case, the algorithm extrapolation to obtain the equivalent cloud cleared radiance is problematic.

We use ~14 yr (1 September 2002–31 March 2016) of version-6 AIRS/AMSU-A level-2 TS and SAT data from the "AIRS/*Aqua* L2 standard physical retrieval (AIRS+AMSU) V006" product (AIRS Science Team/Joao Texeira 2013b). We include all AIRS/AMSU-A observations within 30 km of the point midway between the NOAA station and the GC-Net station at Summit listed in Table 1. We exclude AIRS/AMSU-A temperatures that are flagged as "do not use" by their respective quality control variables.

Although the AIRS/AMSU-A TS is a retrieved quantity, the SAT is calculated by extrapolating the retrieved air temperature profile from the lower troposphere to the surface air pressure SAP obtained from the Global Forecast System. Figure 2 shows that the SAP assumed by the AIRS/AMSU-A algorithm is systematically larger than the surface pressures measured at both stations. The surface pressure assumed by AIRS/AMSU-A may be a correct average over the ~50-km AMSU-A scene used for the retrieval but larger than the pressure measured at Summit, which is a point at a higher elevation. This would also explain the slight increase in the pressure bias with respect to distance from Summit, as increased distances from Summit are also at lower elevations and thus have a higher surface pressure. In addition to variations in surface elevation, surface inhomogeneity in an AIRS/AMSU-A footprint may affect the quality of the AIRS/AMSU-A SAT and TS in Arctic regions such as along coast lines, broken sea ice, and melt ponds over ice. Figure 2 also shows that the GC-Net surface pressure measurements have a larger residual standard error than the NOAA surface pressure measurements, which suggests that the GC-Net sensors have a slightly lower measurement quality. The GC-Net measurements are

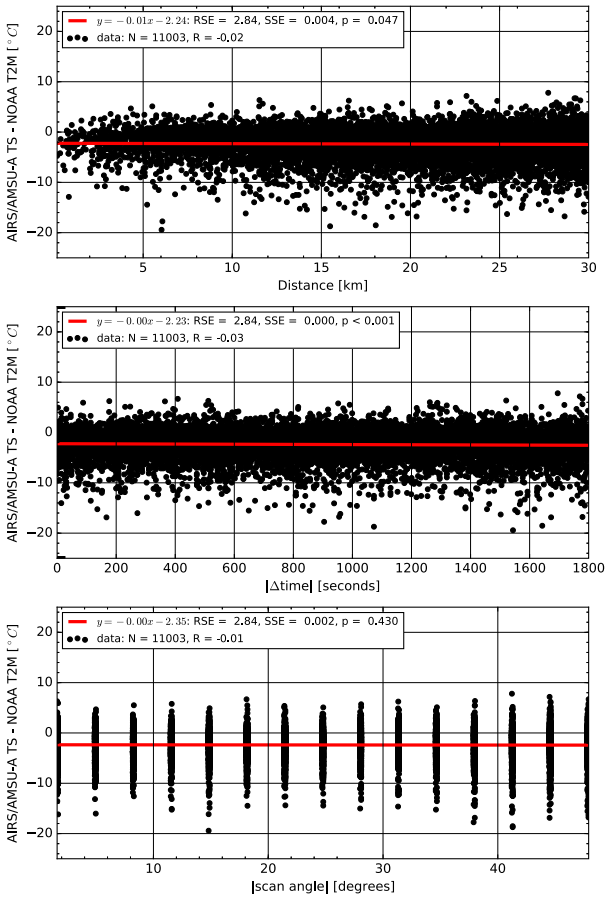

FIG. 7. The AIRS/AMSU-A TS–NOAA T2M difference is shown as a function of the (top) distance of the AIRS observations from the Summit, (middle) offset in time, and (bottom) scan angle of the AIRS observation.

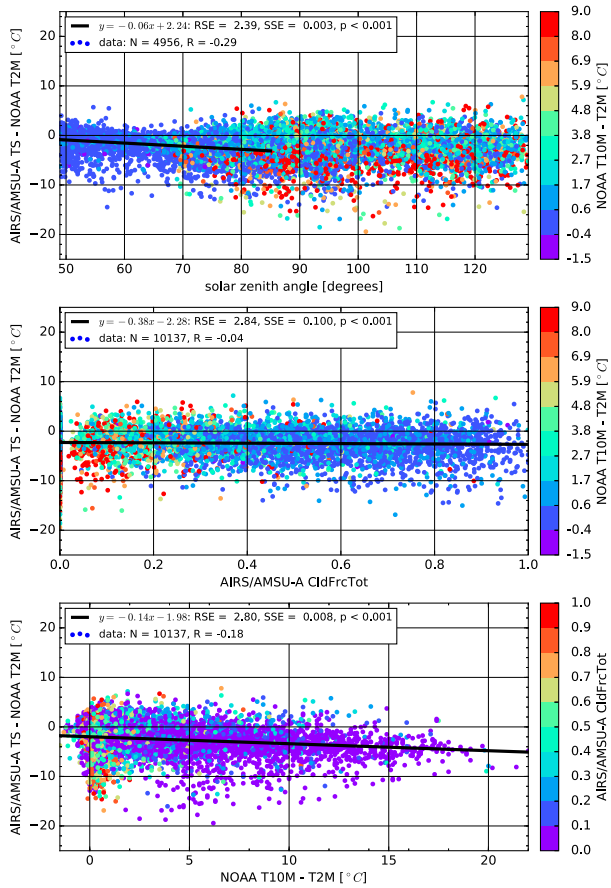

FIG. 8. The AIRS/AMSU-A TS–NOAA T2M difference is compared to the (top) solar zenith angle, (middle) total cloud fraction from AIRS, and (bottom) inversion strength from the NOAA station. The colors in the top and middle panels represent the inversion strength measured by the NOAA T10M–NOAA T2M difference, and the colors in the bottom panel represent the total cloud fraction measured by the AIRS retrieval.

also likely influenced by the vertical displacement of the sensor.

The actual variable names of the TS, SAT, and SAP quantities in the "AIRS/*Aqua* L2 standard physical retrieval (AIRS+AMSU) V006" (AIRS Science Team/Joao Texeira 2013b) are TSurfStd, TSurfAir, and PSurfStd and their corresponding quality control variable names include a "_QC" suffix. In section 3b we examine the difference between the AIRS/AMSU-A and station temperature measurements in terms of various geometrical and environmental quantities including the scan angle from the "AIRS/*Aqua* L2 cloud-cleared infrared radiances (AIRS+AMSU) V006" (AIRS Science Team/Joao Texeira 2013a) and the total cloud fraction and solar zenith angle from the "AIRS/*Aqua* L2 standard physical retrieval (AIRS+AMSU) V006" (AIRS Science Team/Joao Texeira 2013b). The actual variable names of these quantities are scanang, CldFrcTot, and solzen.

c. *MERRA and MERRA-2*

MERRA and MERRA-2 are global, gridded atmospheric reanalyses that assimilate available satellite radiance and conventional observations. The Summit station pressure is assimilated in MERRA and MERRA-2. However, the 2-m temperature and other observed variables from surface stations over land are not assimilated. It is worth noting that neither MERRA nor MERRA-2 assimilates the AIRS/AMSU-A TS data, which makes it an interesting exercise to intercompare MERRA, MERRA-2, AIRS/AMSU-A, and station temperatures. The MERRA/MERRA-2 background atmospheric model is the Goddard Earth Observing System model (GEOS) (Molod et al. 2015). MERRA was produced on a grid with a spacing of 2/3° longitude × 1/2° latitude. MERRA-2 is produced

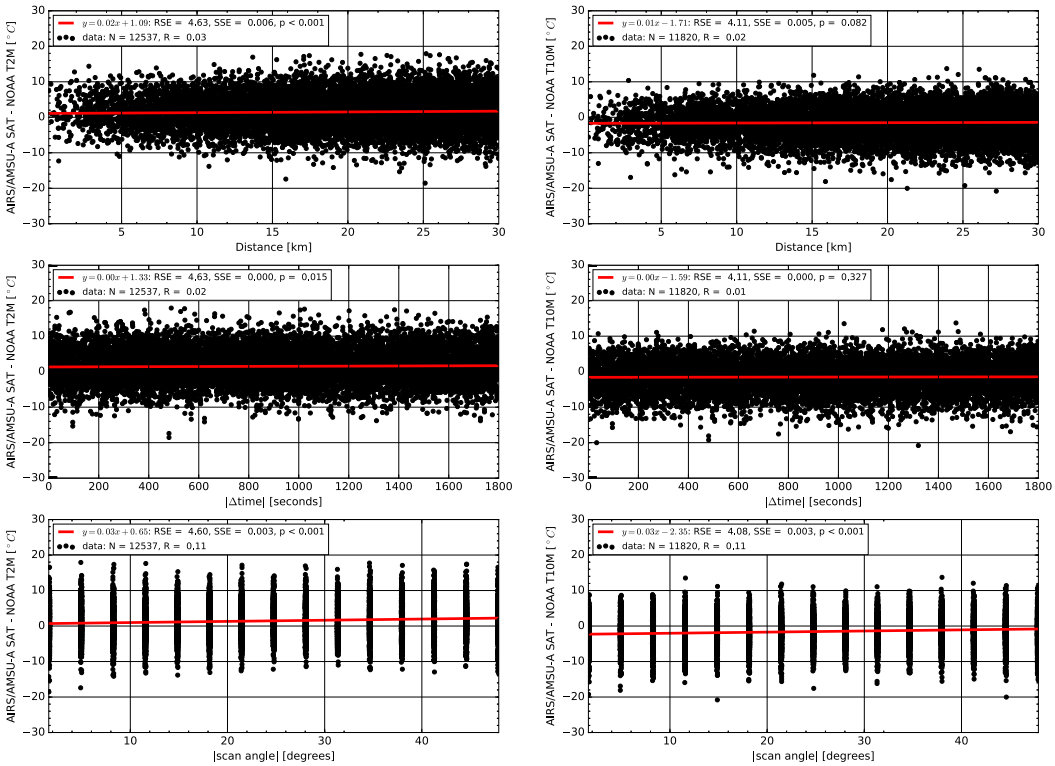

FIG. 9. As in Fig. 7, but comparing SAT to the NOAA (left) T2M and (right) T10M with respect to geometrical factors.

on a similar 5/8° longitude × 1/2° latitude grid, or an approximate spacing of 56 km. Both MERRA and MERRA-2 have 72 vertical levels. The performance of MERRA has been reviewed by Cullather and Bosilovich (2011, 2012). MERRA employed a simplistic representation of the ice sheet surface, including a fixed surface albedo (0.775) and a fixed subsurface (2 m below surface) temperature of 230 K (−43°C). For MERRA-2, the surface representation has been substantially revised to include snow hydrology processes, a prognostic albedo, and energy conductivity through snow and ice layers at high vertical resolution (Cullather et al. 2014). We use T10M, T2M, and TS from the "tavg1_2d_slv_Nx: MERRA 2D IAU diagnostic, single level meteorology, time average 1-hourly V5.2.0" (GMAO 2008) and the "MERRA-2 tavg1_2d_slv_Nx: 2d, 1-hourly, time-averaged, single-level, assimilation, single-level diagnostics V5.12.4" (GMAO 2015).

3. Results

a. Temperature comparisons

We compare near-surface temperature estimates from AIRS/AMSU-A, MERRA, and MERRA-2 with measurements from the NOAA and GC-Net stations at Summit. All temperature estimates have been matched in space to within 30 km of the Summit stations and in time to within 30 min of the AIRS/AMSU-A observations. The linear fit parameters described in this section are summarized both in the figure legends and in Table 2. The AIRS/AMSU-A TS is well correlated with the NOAA T2M ($R = 0.98$) and GC-Net TCAir1 ($R = 0.97$) temperatures (Fig. 3). As with the surface pressure measurements shown in Fig. 2, the temperature measurements shown in Fig. 3 indicate that the temperatures from the GC-Net station have a larger residual standard error than those from the NOAA station possibly because the GC-Net sensors are not held at fixed heights above the surface and they are not shielded. The AIRS/AMSU-A TS tends to be colder than the near-surface air temperature measurements from both stations (Fig. 3). The weather stations probably measure higher temperatures than the surface skin temperature because they are higher in the near-surface temperature inversion.

Although the AIRS/AMSU-A SAT has a slightly better correlation with the NOAA T2M than the NOAA T10M temperature, it is warm with respect to the NOAA T2M temperature during the cold season (Fig. 4). A likely explanation is that the extrapolation of the temperature profile to the surface pressure does not fully account for the strong inversions that occur during

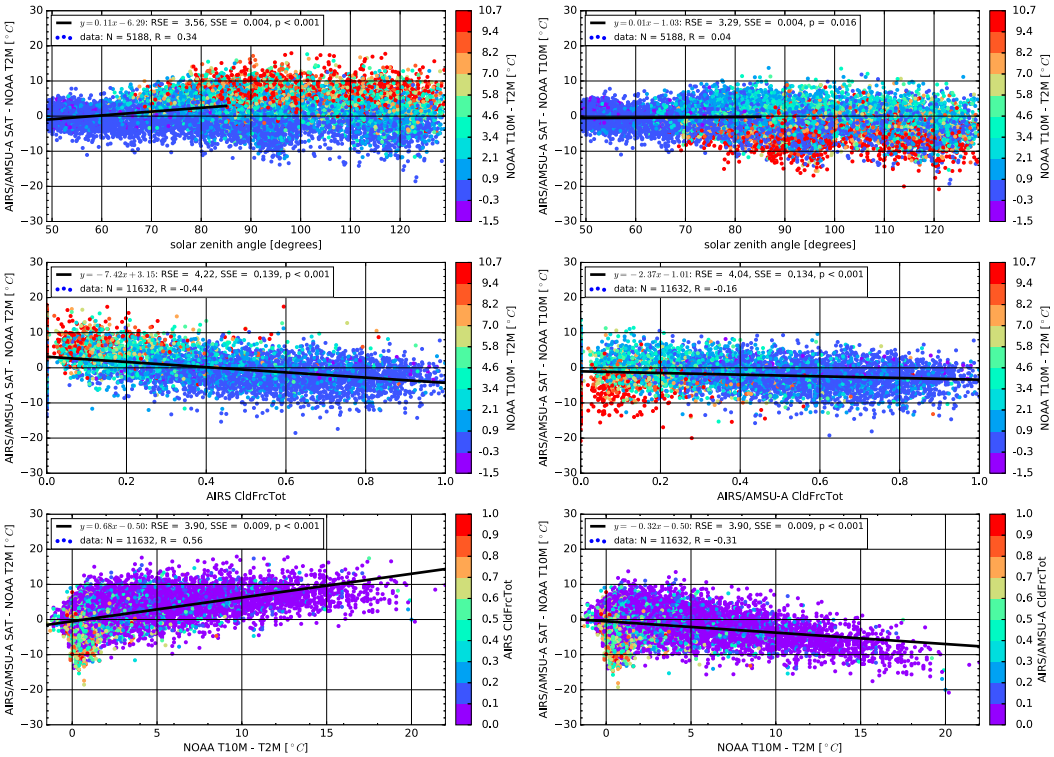

FIG. 10. As in Fig. 8, but comparing SAT to the NOAA (left) T2M and (right) T10M with respect to environmental factors.

the cold season. The AIRS/AMSU-A SAT has a smaller cold season warm bias when compared to the NOAA T10M temperature possibly because the T10M temperature is higher in the boundary layer where AIRS/AMSU-A has more sensitivity. Since the GC-Net temperature sensors are closer together (separation ~1.1 m) than the NOAA sensors (separation 8 m), the correlation with the AIRS/AMSU-A SAT is nearly identical for both temperatures (not shown).

Figures 5 and 6 display temperatures from MERRA Sampled like AIRS/AMSU-A (MSA) and MERRA-2 Sampled like AIRS/AMSU-A (M2SA) compared to station and satellite temperature estimates. The MSA and M2SA T10M and T2M temperatures are compared with the NOAA T10M and T2M temperatures, and the MSA and M2SA TS temperatures are compared with the AIRS/AMSU-A TS temperatures. There appears to be a rotation in the MERRA air temperature differences such that MERRA is biased cold during the warm season and biased warm during the cold season (Fig. 5). The MERRA TS also appears to be biased cold during the warm season but unbiased during the cold season. The MERRA-2 temperatures do not show as much of a rotation as the MERRA temperatures and the MERRA-2 TS has a smaller residual standard error (Fig. 6). The improvements in the MERRA-2 temperatures over MERRA can likely be attributed to the elimination of the fixed subsurface temperature and the representation of energy conduction through the surface in MERRA-2. The fixed subsurface temperature of MERRA tends to artificially pull the surface temperature toward the −43°C value over glaciated land (Cullather et al. 2014). Thus, it appears warm in the cold season and cold in the warm season.

b. *Observing conditions*

Since a previous study found both a scan angle dependence and a solar zenith angle dependence in surface temperature measurements made using MODIS data (Shuman et al. 2014), we decided to examine these and other factors that could explain the observed temperature offsets using AIRS/AMSU-A data. Therefore we examine the differences between the AIRS/AMSU-A TS and the NOAA T2M in terms of *geometrical* and *environmental* observation conditions to find out if AIRS/AMSU-A surface temperature measurements have similar dependencies. The *geometrical* conditions considered are 1) the distance of the AIRS/AMSU-A footprint from the weather station, 2) the difference in time between the AIRS/AMSU-A observation and the hourly average weather station temperature, and

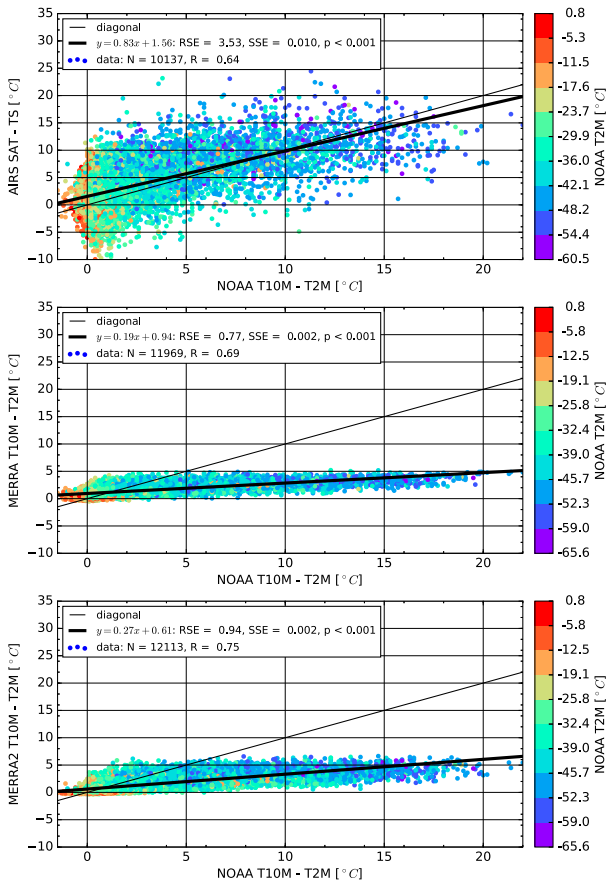

FIG. 11. Several different measures of the near-surface inversion strength are compared to the NOAA T10M − T2M near-surface temperature inversion strength. (top) AIRS SAT − AIRS TS, (middle) MERRA T10M − MERRA T2M, and (bottom) MERRA-2 T10M − MERRA-2 T2M.

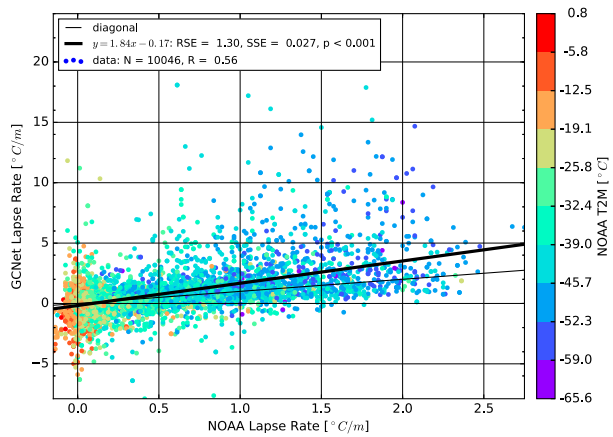

FIG. 12. The lapse rate measured at the NOAA and GC-Net stations. Since the highest GC-Net temperature sensor is usually at ~3 m and the highest NOAA temperature sensor is at 10 m, the figure suggest that the lapse rate is larger closer to the surface. The colors represent the NOAA T2M temperature measurement.

3) the scan angle of the AIRS/AMSU-A observation. The *environmental* conditions we consider are 1) the solar zenith angle, 2) the cloud fraction reported in the AIRS/AMSU-A level-2 product, and 3) the near-surface inversion strength measured by the difference between the NOAA T10M–T2M temperatures. The linear fit parameters described in this section are summarized both in the figure legends and in Table 3.

As previously seen in Fig. 3, Fig. 7 shows that the AIRS/AMSU-A TS tends to be colder than the NOAA T2M. However, there is very little dependence on the distance from Summit, the offset in time, or the scan angle. This suggests a high degree of robustness of AIRS/AMSU-A TS retrievals over a flat snowy surface like Summit with respect to its scan angle and the slope of the surface.

The top panel of Fig. 8 shows that there is a daytime solar zenith angle dependence of the difference between AIRS/AMSU-A TS and the NOAA T2M such that the AIRS/AMSU-A TS–NOAA T2M difference becomes more negative for increasing solar zenith angles. Because the AIRS instrument measures thermal emission, this dependence may partially be an artifact of the increase in the strength of the temperature inversion during the polar night. An encouraging result from the middle panel of Fig. 8 is that the AIRS/AMSU-A TS–NOAA T2M difference has very little ($R = -0.04$) correlation with cloud amount. The bottom panel of Fig. 8 shows AIRS/AMSU-A TS–NOAA T2M as a function of the inversion strength. Although the difference becomes more negative with increasing inversion strength, there are also some cases for which the AIRS/AMSU-A TS is much colder than the NOAA T2M even when the NOAA T10M–T2M suggests a weak inversion. These cases could be due to strong temperature inversions below 2 m that are not captured by the T10M–T2M temperature difference. In section 4a we examine GC-Net data that suggest the lapse rate can sometimes increase as it is closer to the surface.

Figures 9 and 10 are analogous to Figs. 7 and 8 but show the AIRS/AMSU-A SAT–NOAA T2M differences (left panels) and the AIRS/AMSU-A SAT–NOAA T10M differences (right panels). We find little dependence on the geometrical observing conditions (Fig. 9). There is, however, a tendency that the AIRS/AMSU-A SAT is warmer than the NOAA T2M and colder than the NOAA T10M. This may suggest that the AIRS/AMSU-A SAT may be more representative of a temperature somewhere between the 2- and 10-m

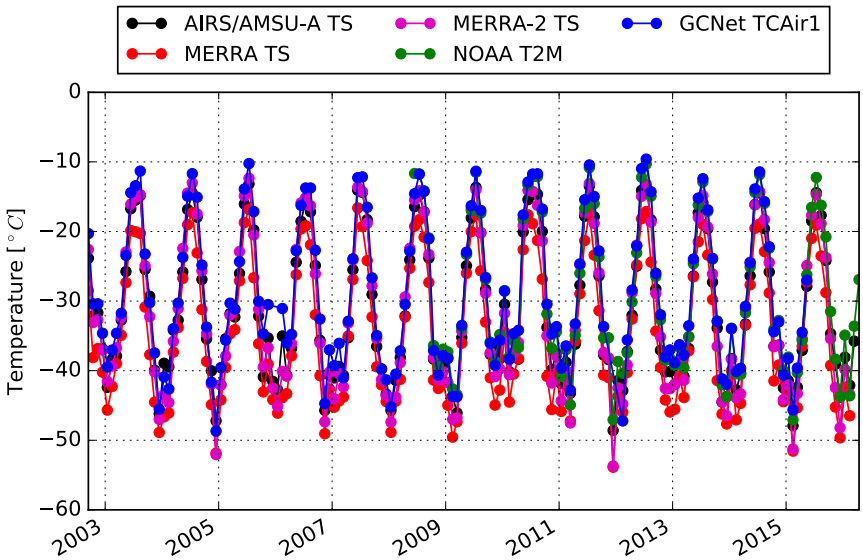

FIG. 13. A time series of monthly mean values of AIRS TS, MERRA and MERRA-2 TS, GC-Net TCAir1, and NOAA T2M.

temperatures. The SAT also seems to have a small scan angle dependence such that observations at larger scan angles tend to be warmer.

The top-left panel of Fig. 10 shows that there is a solar zenith angle dependence in the daytime AIRS/AMSU-A SAT–NOAA T2M temperature differences, while the top-right panel shows that there is almost no solar zenith angle dependence in the daytime AIRS/AMSU-A SAT–NOAA T10M temperature differences. The top panels of Fig. 10 also show that when there are strong temperature inversions at night the AIRS/AMSU-A SAT temperatures tend to be warmer than NOAA T2M temperatures and colder than the NOAA T10M temperatures. The middle panels of Fig. 10 suggest that the AIRS/AMSU-A SAT may have a dependence on clouds, but since the stronger temperature inversions tend to happen when there is a smaller cloud fraction it is more difficult to interpret. The bottom panels of Fig. 10 show that the AIRS/AMSU-A SAT–NOAA T2M difference becomes more positive with increasing inversion strength and the AIRS/AMSU-A SAT–NOAA T10M temperature difference becomes more negative with increasing inversion strength. However, these tendencies may also be influenced by clouds. A possible explanation is that AIRS/AMSU-A temperature profile does not fully resolve the near-surface temperature inversions, and when there is a strong temperature inversion the AIRS/AMSU-A SAT reports a temperature that is somewhere between the 2- and 10-m temperatures.

4. Discussion

a. Inversion strength

Figure 11 compares several different measures of inversion strength to the near-surface inversion strength defined by the difference between the NOAA T10M–T2M temperatures. Although there is a large amount of scatter, the difference between the AIRS/AMSU-A SAT and TS shows sensitivity to the near-surface temperature inversions. The large scatter is likely due to the uncertainty introduced by extrapolating the temperature profile to the surface. Although there are improvements in MERRA-2 temperatures, MERRA and MERRA-2 both often underestimate the near-surface temperature inversions measured at the NOAA Summit station.

Since the GC-Net temperature sensors are usually separated by ~1.1 m and the NOAA temperature sensors are separated by 8 m, we compare the lapse rate derived from the two stations rather than the inversion strength in Fig. 12. Since the GC-Net sensors are usually closer to the surface than the NOAA sensors, Fig. 12 suggests that the lapse rate can be larger closer to the surface. The near-surface component of the temperature inversion may explain the offset between the near-surface air temperature measured at the stations and the surface skin temperature measured by satellite observations.

b. Monthly averages and sampling biases

Figure 13 shows a time series of monthly mean values of AIRS/AMSU-A TS, MERRA and MERRA-2 TS,

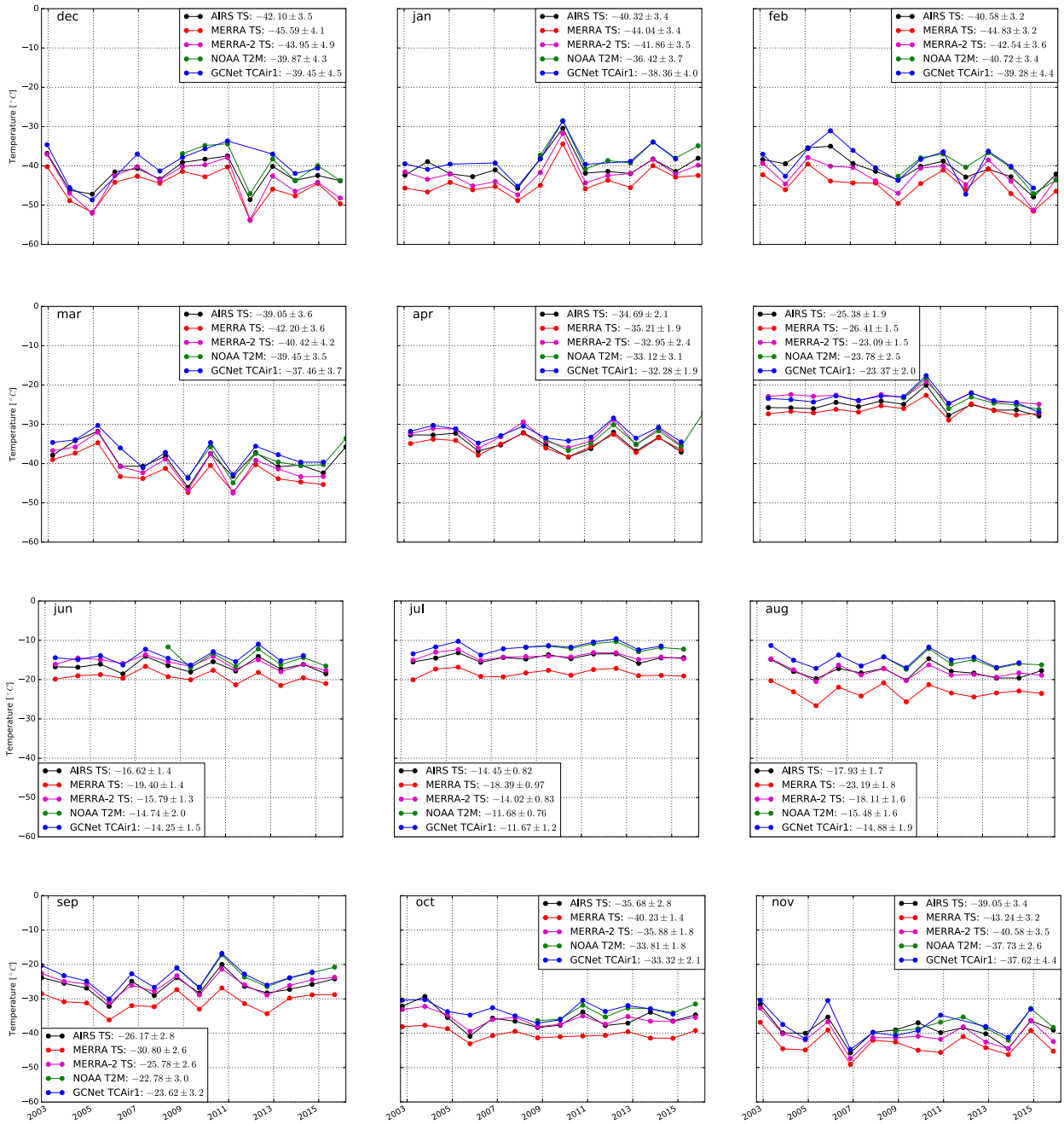

FIG. 14. As in Fig. 13, but with the months separated.

GC-Net TCAir1, and NOAA T2M temperatures. Even neglecting the sampling differences between AIRS/AMSU-A that is sampled ~3–4 times per day and the reanalysis and weather station data that are sampled every hour, Fig. 13 shows that all temperatures agree fairly well on seasonal time scales. Figure 14 shows the same data as Fig. 13 but with the months separated to more easily distinguish the systematic differences for each season. Although there are systematic biases between each of the datasets they are all able to track the relatively warm and cold years. While the AIRS/AMSU-A and MERRA-2 TS estimates tend to be colder than the station near-surface air temperatures, possibly because of the near-surface temperature inversions, the MERRA data tend to be even colder than the AIRS/AMSU-A and MERRA-2 data and thus

TABLE 4. Monthly mean temperatures (°).

Month	AIRS TS	MERRA TS	MERRA-2 TS	NOAA T2M	GCNet TCAir1
Jan	−40.3 ± 3.4	−44.0 ± 3.4	−41.9 ± 3.5	−36.4 ± 3.7	−38.4 ± 4.0
Feb	−40.6 ± 3.2	−44.8 ± 3.2	−42.5 ± 3.6	−40.7 ± 3.4	−39.3 ± 4.4
Mar	−39.1 ± 3.6	−42.2 ± 3.6	−40.4 ± 4.2	−39.5 ± 3.5	−37.5 ± 3.7
Apr	−34.7 ± 2.1	−35.2 ± 1.9	−33.0 ± 2.4	−33.1 ± 3.1	−32.3 ± 1.9
May	−25.4 ± 1.9	−26.4 ± 1.5	−23.1 ± 1.5	−23.8 ± 2.5	−23.4 ± 2.0
Jun	−16.6 ± 1.4	−19.4 ± 1.4	−15.8 ± 1.3	−14.7 ± 2.0	−14.3 ± 1.5
Jul	−14.5 ± 0.8	−18.4 ± 1.0	−14.0 ± 0.8	−11.7 ± 0.8	−11.7 ± 1.2
Aug	−17.9 ± 1.7	−23.2 ± 1.8	−18.1 ± 1.6	−15.5 ± 1.6	−14.9 ± 1.9
Sep	−26.2 ± 2.8	−30.8 ± 2.6	−25.8 ± 2.6	−22.8 ± 3.0	−23.6 ± 3.2
Oct	−35.7 ± 2.8	−40.2 ± 1.4	−35.9 ± 1.8	−33.8 ± 1.8	−33.3 ± 2.1
Nov	−39.1 ± 3.4	−43.2 ± 3.2	−40.6 ± 3.5	−37.7 ± 2.6	−37.6 ± 4.4
Dec	−42.1 ± 3.5	−45.6 ± 4.1	−44.0 ± 4.9	−39.9 ± 4.3	−39.5 ± 4.5

likely have a cold measurement bias. Table 4 lists the monthly mean values for the temperatures displayed in Fig. 14. The differences can be attributed to both measurement differences, errors, and sampling biases.

Sampling can be important. For example, Figs. 13 and 14 both show a spike in the monthly mean temperature of the GC-Net TCAir1 in February 2006 because most of the observations are missing for that month. The Summit stations are located nearly at the highest elevation in Greenland, thus they are typically colder than the surrounding land, which is at lower altitudes but is also included in the AIRS/AMSU-A ~50-km footprint. We expect that the sampling bias may be even greater in the AIRS/AMSU-A level-3 product than the estimates shown here because the level-3 product includes all observations within 1 square degree. The larger area averaged over in the level-3 product includes even more observations at lower elevation than are included within the 30-km radius used for the spatial matchup in this study.

We expect that the atmospheric state can have a larger impact on the sampling bias than the size of the AMSU-A footprint. Since certain scenes (e.g., uniformly cloudy) are rejected by the quality control, the AIRS/AMSU-A observations can have scene dependent sampling biases. The sampling bias can be estimated using correlative datasets not subject to the same sampling effects (e.g., Hearty et al. 2014) by subtracting an unbiased average of the correlative dataset from an average with the same sampling as the satellite observations. Figure 15 shows the yield of AIRS/AMSU-A observations at Summit in the top panel. We define the yield as the number of accepted observations divided by the number of attempted observations. The bottom panel of Fig. 15 shows the sampling bias of monthly mean AIRS/AMSU-A TS observations estimated using MERRA, MERRA-2, and the NOAA and GC-Net station observations. Although the yield of the AIRS/AMSU-A TS is usually very high (>90%) at Summit, in January and February it can be <50%. The drops in yield during the winter season correspond with increases in the sampling bias estimates up to ~4°C using both the reanalyses and the station measurements.

Figure 16 is the same as Fig. 15 but with the months separated to more easily distinguish the systematic sampling biases for each month. Table 5 lists the yield and the mean sampling bias estimates for the AIRS/AMSU-A TS derived from each of the correlative datasets. During the warm months, the MERRA-derived sampling bias estimate is colder than the estimates derived from the other observations. Therefore the cold

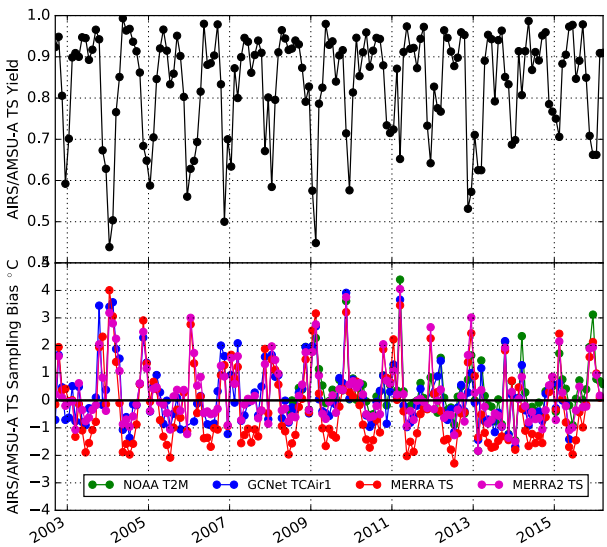

FIG. 15. (top) A time series of the monthly yield in the AIRS observations at the Greenland Summit. (bottom) A time series of estimates of the AIRS sampling bias using MERRA, MERRA-2, and the NOAA and GC-Net station observations.

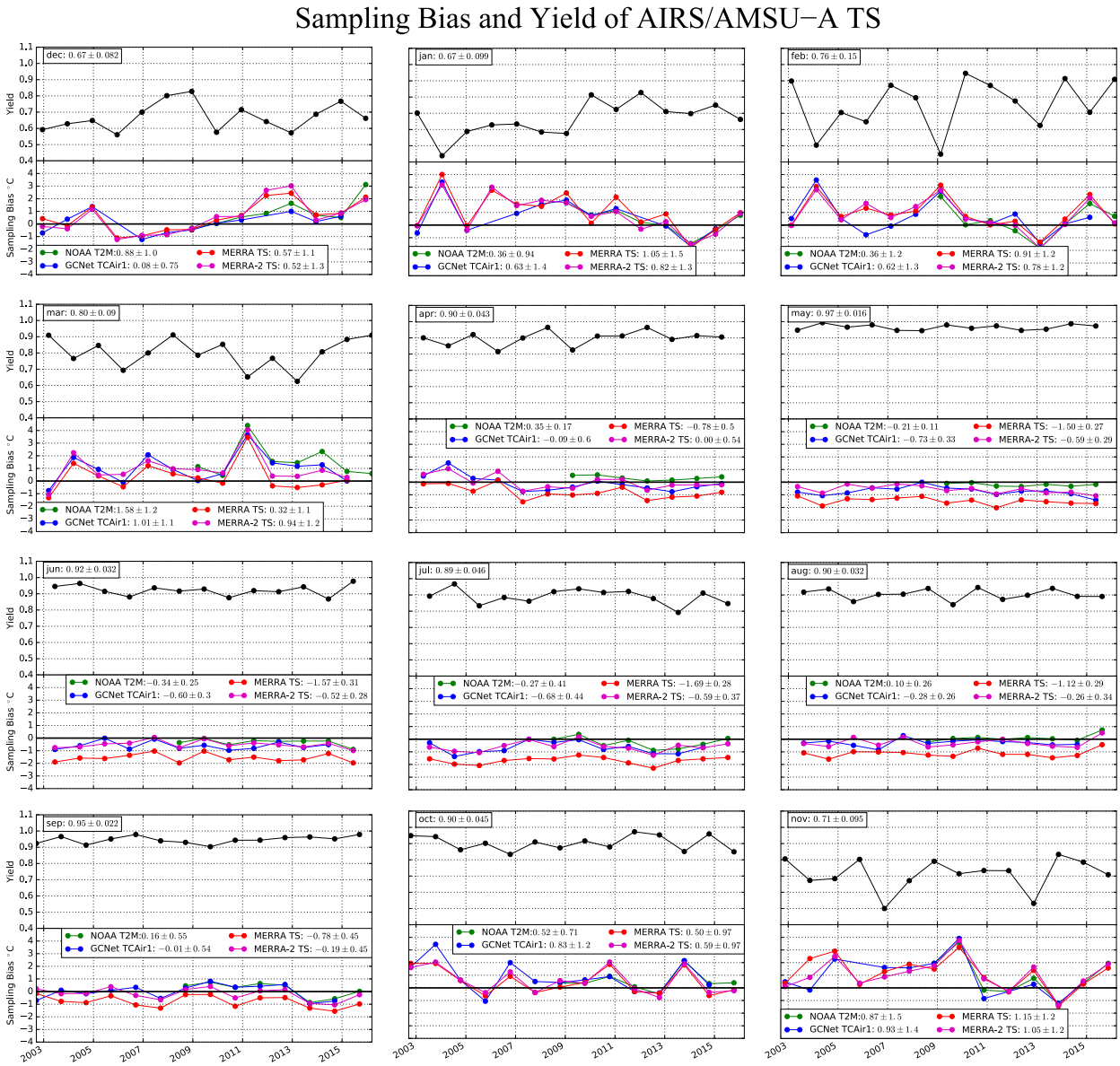

FIG. 16. As in Fig. 15, but with the months separated.

sampling bias inferred from the MERRA data during the warm season is likely spurious.

c. *Summer of 2012*

The summer of 2012 showed unprecedented warming over Greenland such that melting was observed at Summit (Tedesco et al. 2013). Both the NOAA and GC-Net stations reported near-surface air temperatures above 0° (e.g., Fig. 3). Although neither the SAT nor the TS observed by AIRS/AMSU-A rose above freezing, there were changes in the microwave emissivity that suggest a phase transition was taking place. The AIRS/AMSU-A level-2 product includes a microwave surface class that classifies the surface type as "coastline," "land," "ocean," "sea ice," "snow," or "glacier" based on an ad hoc algorithm using the brightness temperatures from AMSU-A channels 1 (23.8 GHz), 2 (31.4 GHz), and 15 (89.0 GHz). For this brief period during the summer of 2012, the microwave surface class indicated that the Summit was "land." The measurements identified as land appear as red dots in Fig. 3 and correspond to times when the air temperatures measured at the stations were near or above the freezing point of water. These erroneous land classifications were likely the result of a phase transition in the ice at the Summit. Grody (1988) has shown that the emissivity of

TABLE 5. Yield and sampling bias estimates.

Month	Yield	NOAA T2M (°)	GCNet TCAir1 (°)	MERRA TS (°)	MERRA-2 TS (°)
Jan	0.67 ± 0.10	0.36 ± 0.94	0.63 ± 1.4	1.05 ± 1.5	0.82 ± 1.3
Feb	0.76 ± 0.15	0.36 ± 1.2	0.62 ± 1.3	0.91 ± 1.2	0.78 ± 1.2
Mar	0.80 ± 0.09	1.58 ± 1.2	1.01 ± 1.1	0.32 ± 1.1	0.94 ± 1.2
Apr	0.90 ± 0.04	0.35 ± 0.17	−0.09 ± 0.6	−0.78 ± 0.5	0.00 ± 0.54
May	0.97 ± 0.01	−0.21 ± 0.11	−0.73 ± 0.33	−1.50 ± 0.27	−0.59 ± 0.29
Jun	0.92 ± 0.32	−0.34 ± 0.25	−0.60 ± 0.3	−1.57 ± 0.31	−0.52 ± 0.28
Jul	0.89 ± 0.46	−0.27 ± 0.41	−0.68 ± 0.44	−1.69 ± 0.28	−0.59 ± 0.37
Aug	0.90 ± 0.03	0.10 ± 0.26	−0.28 ± 0.26	−1.12 ± 0.29	−0.26 ± 0.34
Sep	0.95 ± 0.22	0.16 ± 0.55	−0.01 ± 0.54	−0.78 ± 0.45	−0.19 ± 0.45
Oct	0.90 ± 0.05	0.52 ± 0.71	0.83 ± 1.2	0.50 ± 0.97	0.59 ± 0.97
Nov	0.71 ± 0.10	0.87 ± 1.5	0.93 ± 1.4	1.15 ± 1.2	1.10 ± 1.2
Dec	0.67 ± 0.08	0.9 ± 1.0	0.08 ± 0.8	0.57 ± 1.1	0.52 ± 1.3

wet snow is much higher and has a spectral shape more like that of *land* than of *dry* or *refrozen snow*. The change in the microwave emissivity during this period is easily apparent in a time series of any of the AMSU-A channels (e.g., Fig. 17). We will further examine the changes in microwave emissivity associated with this event in a subsequent paper.

5. Summary and conclusions

We have compared ~14 yr of AIRS/AMSU-A, MERRA, and MERRA-2 near-surface air and skin temperature estimates with NOAA and GC-Net station measurements at Summit, Greenland. The GC-Net station measurements have a larger standard error than the NOAA station measurements. The AIRS/AMSU-A TS tends to be colder than the near-surface air temperatures likely because of the near-surface temperature inversions present in the Arctic.

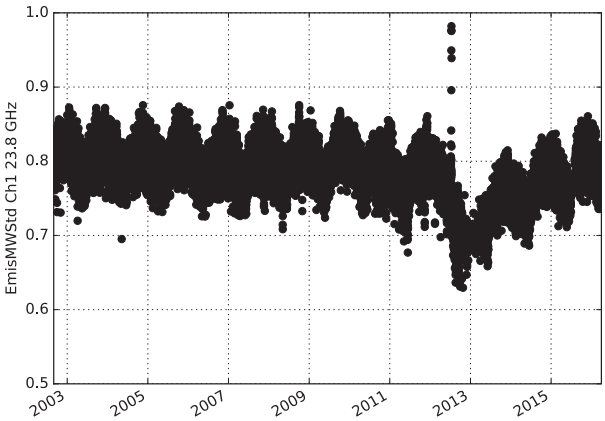

FIG. 17. A time series of the AMSU-A channel 1 (23.8 GHz) emissivity at Summit clearly shows the melting event in the summer of 2012.

We also find that the sampling bias of AIRS/AMSU-A observations may be warm by as much as 4°C during the polar night. Therefore, gridded products such as the AIRS/AMSU-A level-3 TS should be used with caution when interpreting absolute temperature measurements in this region during the polar night. Although the difference between the AIRS/AMSU-A SAT and TS shows some skill in predicting temperature inversions, the SAT may not provide sufficient sensitivity in the lowest part of the inversion layer. Because the AIRS/AMSU-A SAT is defined as the extrapolation of the temperature profile to the surface pressure, it may carry too much memory of temperatures higher in the atmosphere than the automatic weather stations. This may particularly be the case when there is a strong near-surface temperature inversion. We also find that the AMSU-A instrument shows some sensitivity to the change in emissivity associated with the melting that occurred at Summit, Greenland, during the summer of 2012. Using the AIRS/AMSU-A TS and NOAA T2M and T10M temperatures all of which are not assimilated by MERRA/MERRA-2, we find that the MERRA-2 TS, T2M, and T10M temperatures show improvements over the MERRA temperatures but with little sensitivity to temperature inversions. As a caveat, the AIRS/AMSU-A surface temperature measurements over Greenland should be used with caution in other regions where surface inhomogeneity is large and dynamic (e.g., coast lines, broken sea ice, melt ponds over ice) within an AMSU-A footprint. Further validation is needed to quantify the impact of these surface conditions on the retrieved surface temperature. Further validation is also necessary for the AIRS infrared-only TS algorithm that does not use the AMSU-A instrument.

Acknowledgments. We thank Christopher Shuman for his insights on the Greenland station observations and three anonymous reviewers for numerous suggestions to

improve this paper. The MERRA, MERRA-2, and AIRS/AMSU-A data products were obtained from the Goddard Earth Sciences Data and Information Services Center (GES DISC). Authors JL, DW, RC, and SN are supported by the NASA Interdisciplinary Research in Earth Science (IDS) program (NNH12ZDA001N-IDS). Author RC is also supported by the NASA Modeling, Analysis, and Prediction (MAP) program (NNH12ZDA001N-MAP).

REFERENCES

AIRS Science Team/Joao Texeira, 2013a: AIRI2CCF: AIRS/*Aqua* L2 cloud-cleared infrared radiances (AIRS+AMSU) V006. GES DISC, accessed 29 April 2016, https://doi.org/10.5067/AQUA/AIRS/DATA204.

——, 2013b: AIRX2RET: AIRS/*Aqua* L2 standard physical retrieval (AIRS+AMSU) V006. GES DISC, accessed 29 April 2016, https://doi.org/10.5067/AQUA/AIRS/DATA201.

Alley, R. B., and I. Joughin, 2012: Modeling ice-sheet flow. *Science*, **336**, 551, https://doi.org/10.1126/science.1220530.

Aumann, H. H., and Coauthors, 2003: AIRS/AMSU/HSB on the *Aqua* mission: Design, science objectives, data products, and processing systems. *IEEE Trans. Geosci. Remote Sens.*, **41**, 253–264, https://doi.org/10.1109/TGRS.2002.808356.

Bindschadler, R. A., and Coauthors, 2013: Ice-sheet model sensitivities to environmental forcing and their use in projecting future sea level (the SeaRISE project). *J. Glaciol.*, **59**, 195–224, https://doi.org/10.3189/2013JoG12J125.

Boisvert, L. N., J. N. Lee, J. T. M. Lenaerts, B. Noël, M. R. van den Broeke, and A. W. Nolin, 2017: Using remotely sensed data from AIRS to estimate the vapor flux on the Greenland ice sheet: Comparisons with observations and a regional climate model. *J. Geophys. Res. Atmos.*, **122**, 202–229, https://doi.org/10.1002/2016JD025674.

Bosilovich, M. G., S. Akella, L. Coy, R. Cullather, C. Draper, and R. Gelaro, 2016: MERRA-2: Initial evaluation of the climate. NASA Tech. Rep. Series on Global Modeling and Data Assimilation, Vol. 43, R. D. Koster, Ed., NASA/TM-2015-104606, 145 pp., https://gmao.gsfc.nasa.gov/pubs/docs/Bosilovich803.pdf.

Cullather, R. I., and M. G. Bosilovich, 2011: The moisture budget of the polar atmosphere in MERRA. *J. Climate*, **24**, 2861–2879, https://doi.org/10.1175/2010JCLI4090.1.

——, and ——, 2012: The energy budget of the polar atmosphere in MERRA. *J. Climate*, **25**, 5–24, https://doi.org/10.1175/2011JCLI4138.1.

——, S. M. J. Nowicki, B. Zhao, and M. J. Suarez, 2014: Evaluation of the surface representation of the Greenland ice sheet in a general circulation model. *J. Climate*, **27**, 4835–4856, https://doi.org/10.1175/JCLI-D-13-00635.1.

Devasthale, A., U. Willén, K.-G. Karlsson, and C. G. Jones, 2010: Quantifying the clear-sky temperature inversion frequency and strength over the Arctic Ocean during summer and winter seasons from AIRS profiles. *Atmos. Chem. Phys.*, **10**, 5565–5572, https://doi.org/10.5194/acp-10-5565-2010.

GMAO, 2008: MAT1NXSLV: tavg1_2d_slv_Nx: MERRA 2D IAU diagnostic, single level meteorology, time average 1-hourly V5.2.0. GES DISC, accessed 29 April 2016, https://doi.org/10.5067/B6DQZQLSFDLH.

——, 2015: M2T1NXSLV: MERRA-2 tavg1_2d_slv_Nx: 2d, 1-hourly, time-averaged, single-level, assimilation, single-level diagnostics V5.12.4. GES DISC, accessed 29 April 2016, https://doi.org/10.5067/VJAFPLI1CSIV.

Grody, N. C., 1988: Surface identification using satellite microwave radiometers. *IEEE Trans. Geosci. Remote Sens.*, **26**, 850–859, https://doi.org/10.1109/36.7716.

Hall, D. K., R. S. Williams, S. B. Luthcke, and N. E. Digirolamo, 2008: Greenland ice sheet surface temperature, melt and mass loss: 2000–06. *J. Glaciol.*, **54**, 81–93, https://doi.org/10.3189/002214308784409170.

——, J. C. Comiso, N. E. Digirolamo, C. A. Shuman, J. E. Box, and L. S. Koenig, 2013: Variability in the surface temperature and melt extent of the Greenland ice sheet from MODIS. *Geophys. Res. Lett.*, **40**, 2114–2120, https://doi.org/10.1002/grl.50240.

Hearty, T. J., and Coauthors, 2014: Estimating sampling biases and measurement uncertainties of AIRS/AMSU-A temperature and water vapor observations using MERRA reanalysis. *J. Geophys. Res. Atmos.*, **119**, 2725–2741, https://doi.org/10.1002/2013JD021205.

McGrath, D., W. Colgan, N. Bayou, A. Muto, and K. Steffen, 2013: Recent warming at Summit, Greenland: Global context and implications. *Geophys. Res. Lett.*, **40**, 2091–2096, https://doi.org/10.1002/grl.50456.

Molod, A., L. Takacs, M. Suarez, and J. Bacmeister, 2015: Development of the GEOS-5 atmospheric general circulation model: Evolution from MERRA to MERRA2. *Geosci. Model Dev.*, **8**, 1339–1356, https://doi.org/10.5194/gmd-8-1339-2015.

Parkinson, C. L., 2003: *Aqua*: An Earth-observing satellite mission to examine water and other climate variables. *IEEE Trans. Geosci. Remote Sens.*, **41**, 173–183, https://doi.org/10.1109/TGRS.2002.808319.

Rienecker, M. M., and Coauthors, 2011: MERRA: NASA's Modern-Era Retrospective Analysis for Research and Applications. *J. Climate*, **24**, 3624–3648, https://doi.org/10.1175/JCLI-D-11-00015.1.

Shuman, C. A., D. K. Hall, N. E. DiGirolamo, T. K. Mefford, and M. J. Schnaubelt, 2014: Comparison of near-surface air temperatures and MODIS ice-surface temperatures at Summit, Greenland (2008–13). *J. Appl. Meteor. Climatol.*, **53**, 2171–2180, https://doi.org/10.1175/JAMC-D-14-0023.1.

Steffen, K., J. E. Box, and W. Abdalati, 1996: Greenland climate network: GC-Net. Glaciers, ice sheets and volcanoes: A Tribute to Mark F. Meier, S. C. Colbeck, Ed., CRREL Special Rep. 96-27, 98–103.

Susskind, J., J. M. Blaisdell, and L. Iredell, 2014: Improved methodology for surface and atmospheric soundings, error estimates, and quality control procedures: The Atmospheric Infrared Sounder Science Team version-6 retrieval algorithm. *J. Appl. Remote Sens.*, **8**, 084994, https://doi.org/10.1117/1.JRS.8.084994.

Tedesco, M., X. Fettweis, T. Mote, J. Wahr, P. Alexander, J. E. Box, and B. Wouters, 2013: Evidence and analysis of 2012 Greenland records from spaceborne observations, a regional climate model and reanalysis data. *Cryosphere*, **7**, 615–630, https://doi.org/10.5194/tc-7-615-2013.

Zwally, H. J., W. Abdalati, T. Herring, K. Larson, J. Saba, and K. Steffen, 2002: Surface melt-induced acceleration of Greenland ice-sheet flow. *Science*, **297**, 218–222, https://doi.org/10.1126/science.1072708.